

PLANAR CHANNELING EFFECTS IN A BATCH PROCESS ION IMPLANTER

Reuel B. LIEBERT, Daniel F. DOWNEY, and Vijay K. BASRA

Varian Associates/Extrion Division, Gloucester, MA 01930, USA

In batch process implantation systems, the presence of platen rotation and the possible use of domed platens produce averaging effects which complicate the design of implant geometries to minimize channeling. Data is presented for both flat and domed platens with different wafer orientation (twist) angles. Evidence is shown that channeling effects can be equivalently reduced for both flat and domed geometries.

1. Introduction

In recent years, considerable interest has been generated in techniques for the elimination or reduction of ion beam channeling effects during ion implantation [1-5]. Axial channeling is typically avoided by tilting the wafers 7° to 10° from normal incidence. The usual angles introduced by electrostatic scan systems and domed platens typically do not produce axial channeling problems, but can introduce nonuniformity effects [4,6].

Planar channeling has been studied experimentally [4-5,7-9] on both silicon and GaAs wafers. It has been found to produce variations in sheet resistance uniformity and corresponding junction depth changes in a variety of low dose applications. In the case of the batch process implanters, the analysis becomes clouded because the implant geometry introduces averaging of crystal incidence angles. The geometry variables for disc-based machines are:

- (a) Implant angle (tilt) of the beam.
- (b) Wafer orientation relative to disc axes.
- (c) Platen doming (flex angle).
- (d) Platen angle with respect to disc spin axis.
- (e) Slow scan trajectory and plane relative to wafers.
- (f) Angular variation in the incident beam.

This paper investigates the effects of (b), (c) for the case of a fixed 7.5° implant angle, with the platen parallel to the disc surface (perpendicular to the spin axis), and the scan plane parallel to the disc surface. The scan is obtained with a magnetic system described elsewhere [10] and provides a beam whose nominal angle is constant with respect to the disc surface during the scan. All data was taken, on a Model 160-10 Varian/Extrion Ion Implantation system [11] using 125 mm wafers.

2. Experimental arrangement

In any implantation system, the sheet resistance patterns which are measured on implanted wafers are affected by several phenomena other than channeling. These include alignment errors, machining tolerances, processing-induced nonuniformity, projected area effects on curved surfaces, etc.. The 160-10 system allows these effects to be corrected in the direction of slow scan; wafer probing results are used to directly adjust the scan rate to compensate for observed nonuniformity [12]. This technique will, in normal use, remove some channeling-induced nonuniformity as well as geometrical effects.

In the present study, wafers of (100) orientation with 280-320 Å oxide coatings were prepared for use in the scan correction procedure. The standard implant chosen was $7E13$ atoms/cm² of B⁺ dopant ions at 50 keV energy. Dopant loss in the oxide coatings is 0.44% at 300 angstroms (using LSS range statistics). Wafers in each oxide lot were separated for thickness measurements using a Nanometrics #101 micro-area gauge. Results varied from 1.0 to 3.5% standard deviations. The net effect of the oxide on the dopant uniformity was, therefore, negligible except for the reduction in channeling. The scan correction customization process described in [12] was applied to these oxide wafers after processing. Furnace anneals were done in nitrogen at 900°C for 30 min, and all wafer probing was done on a Prometrix Omniprobe #111C four-point probe system. Followup implants were run to verify the effectiveness of the scan correction process. Figs. 1a, 1b show the results of scan corrections done for domed and flat platens, respectively.

When the scan corrections are applied to bare wafers, the resulting sheet resistance nonuniformity patterns are dominated by channeling effects. The wafers were loaded individually into the implant disc using a fixture designed to control the wafer flat orientation to within

IMPLANT CUSTOMIZATION

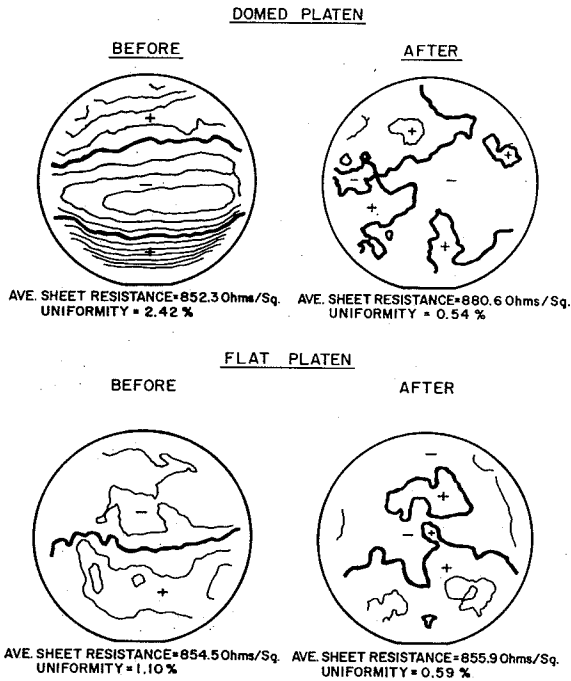


Fig. 1. Results of scan pattern customization on oxide wafers implanted on domed and flat platens.

less than 0.5°. Orientation of the flat radially outward was defined as zero twist angle. The scan corrections were made at 0° twist on the oxide wafers, and runs were made for each twist angle at the same implant

conditions for 0°–55° in 5° intervals on bare wafers. The implants were made on both domed and flat platens using a single row disc.

After each domed platen implant, a wafer was left unannealed and several of these were analyzed using the SIMS technique.

3. Results

Typical wafers at each angle are shown in figs. 2 and 3. The wafer maps are constructed using 625 point mapping and software supplied with the prober. The arrows under each wafer show the radially outward (slow scan) direction. Detailed data for sheet resistance and uniformity are given in table 1. The sheet resistance values are averages of the 625 wafer points averaged over two wafers per angle. Uniformities are single standard deviation values as obtained directly from the prober. The value of the sheet resistance at the wafer center is also provided in the table (again averaged over two wafers).

The variation of sheet resistance with twist angle is shown graphically in fig. 4. The curves have been normalized to each other at 30° to illustrate the relative variations of domed and flat platens. Fig. 5 illustrates the variation of sheet resistance uniformity as a function of twist angle. For both graphs the curves are drawn only to guide the eye, but they are constrained to keep within experimental error of the data points with the smoothest variation possible.

Figs. 6a, b and c illustrate the as-implanted SIMS profiles obtained from implants on domed platens at 0°, 30° and 50°, respectively. The two profiles on each

DOMED PLATEN WAFER MAPS

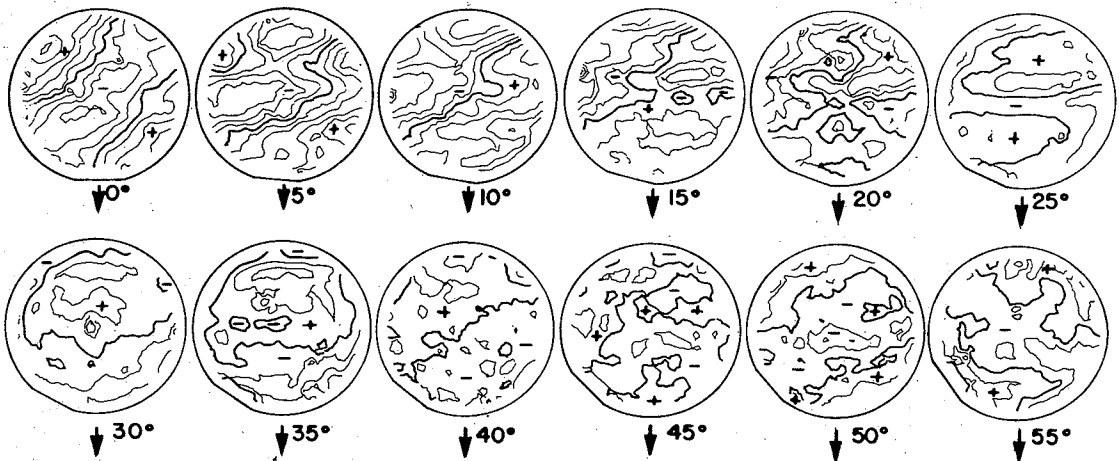


Fig. 2. Sheet resistance contour maps derived from four-point probe data on wafers implanted on domed platens as a function of twist angle. The arrows indicate the direction of slow scan for each wafer.

FLAT PLATEN WAFER MAPS

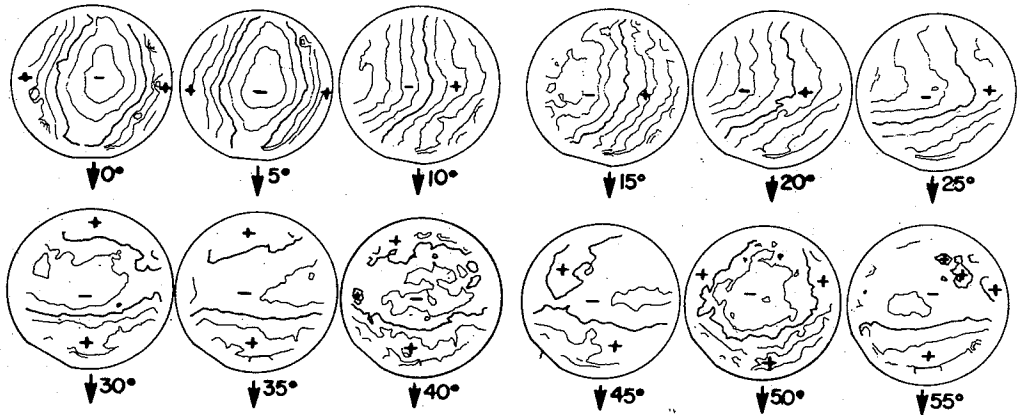


Fig. 3. Sheet resistance contour maps derived from four-point probe data on wafers implanted on flat platens as a function of twist angle. The arrows indicate the direction of slow scan for each wafer.

graph were chosen to show the maximum shoulder difference. The shoulder contribution Δx (1/10) was estimated by measuring the point at which the peak concentration dropped by a factor of 10, and noting this point's separation from the peak concentration depth. The junction depth was also estimated from these curves, using a $5E15$ atoms/cm³ baseline. The results of the analysis are also given in figs. 6a, b and c.

Table 1.

Summary of sheet resistance data on bare wafers for domed and flat platens. All twist angles are in degrees and sheet resistances are in Ω/\square . Uniformities are calculated as single standard deviations of the sheet resistance distribution on a wafer (625 points). Two wafer averages are used for each data point.

Twist angle (degree)	Domed platens			Flat platens		
	R_{avg}	R_{ctr}	σ (%)	R_{avg}	R_{ctr}	σ (%)
0	823.90	802.90	2.32	805.12	785.05	1.64
5	842.80	824.75	2.39	797.49	773.27	1.76
10	855.40	849.38	2.34	808.17	794.04	2.49
15	874.36	872.95	1.69	819.49	817.80	2.39
20	882.75	889.80	1.12	831.09	823.66	2.02
25	883.38	880.30	0.90	847.06	840.20	1.53
30	874.29	880.65	0.98	848.57	837.08	1.19
35	877.59	875.50	1.17	859.42	853.12	0.94
40	885.59	884.75	0.80	844.77	825.98	1.05
45	866.63	865.35	0.71	846.45	839.31	0.69
50	864.24	845.97	0.89	844.81	828.00	1.21
55	862.55	857.35	0.82	852.90	845.47	0.88

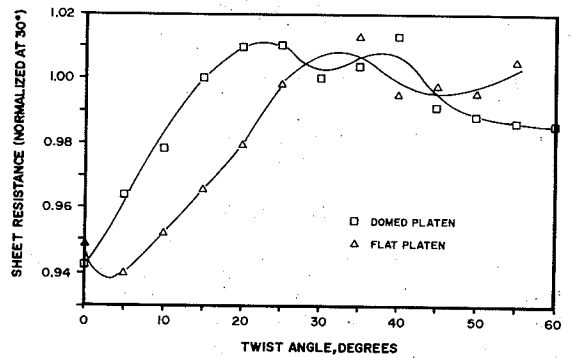


Fig. 4. Variation of sheet resistance with twist angle for wafers implanted on domed and flat platens. The data have been normalized at 30°. The curves are drawn solely to guide the eye, and should not be understood to represent channeling behavior in detail.

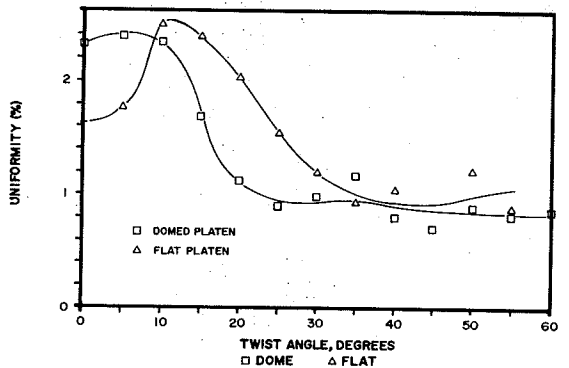


Fig. 5. Variation of sheet resistance uniformity with twist angle for wafers implanted on domed and flat platens. The uniformity is expressed as a standard deviation of the sheet resistance from a 625 point probe map.

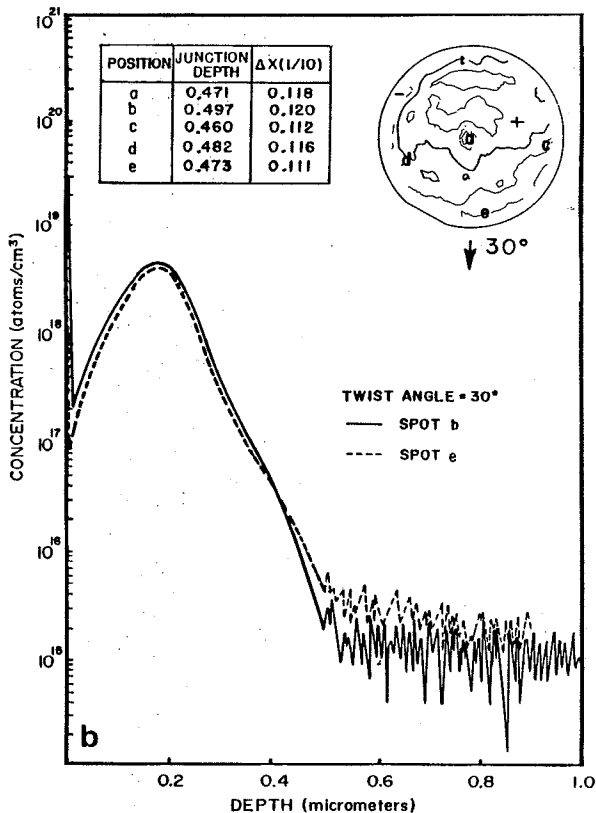
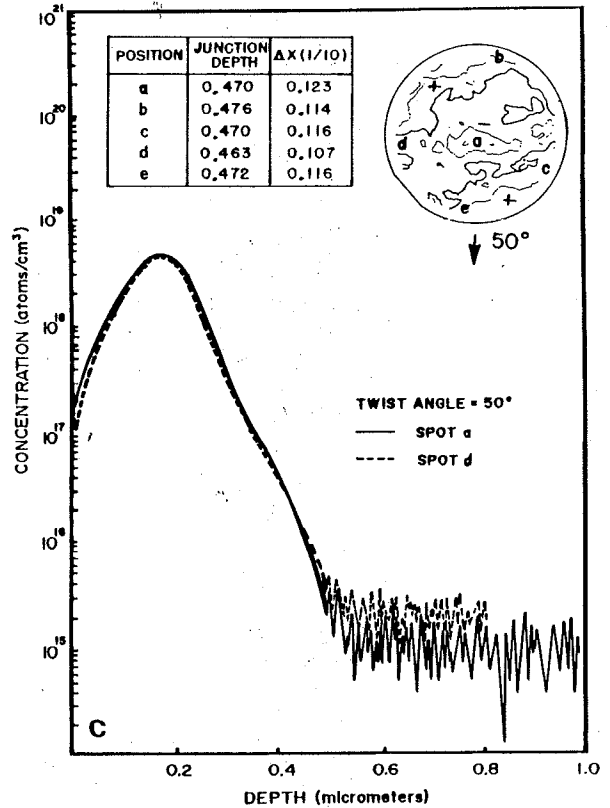
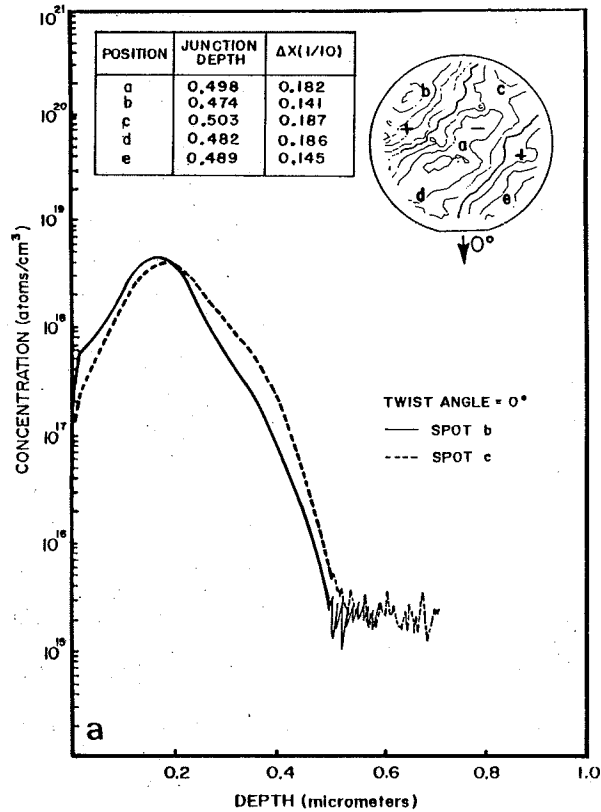


Fig. 6. Overlay of as-implanted SIMS profiles at points showing minimum and maximum channeling effect. Map shows points selected for SIMS analysis, and junction depths are obtained at the $5E15$ atoms/cm³ baseline level. The distances are given in μm and angles in degrees. The $\Delta x(1/10)$ values are distances from the peak concentration to the 1/10 value point, and are a measure of the channeling shoulder. The overlays are of wafers implanted on a domed platen at (a) 0°, (b) 30° and (c) 50° twist angle.

4. Analysis

The sheet resistance patterns in figs. 2 and 3 show substantial differences between domed and flat platens, and both figures show improvement as the twist angle is increased.

The sheet resistance curves in fig. 4 show that the domed platen rises more quickly to its asymptotic (least channeled) value than the equivalent flat platen curve, but both are comparable above 30°.

In fig. 5, it is seen that the domed platen uniformity is considerably worse than the flat platen result at 0°. The domed data, however, initially improves with increased twist angle, while the flat platen uniformity worsens. By the time 30° is reached, the uniformity results are equal, and remain that way as the twist angle continues to rise.

The SIMS data tabulated in figs. 6a–6c verifies the strong channeling contribution at zero degrees. The shoulder depths differ by $0.04\ \mu\text{m}$ between different points on the same wafer, and the shallowest shoulders are $0.14\ \mu\text{m}$ from the peak. The data at 30° and 50° , however, show no major differences between shoulders at different points (within the depth precision), and the shoulders are typically 0.11 to 0.12 from the peak.

It is clear that the present data show no advantage to be had in channeling elimination from using flat platens. As long as wafer twist orientation will be performed to minimize planar channeling, either platen geometry will give similar results. The twist angle rotates by $+/-12^\circ$ as the fast scan is performed for both domed and flat platens. The tilt angle will vary over a spread of 2.5° from the 7.5° standard for the domed platens only. Analytical work is in process to correlate the angular variations of beam incidence relative to crystal planes with specific map structures observed on the wafers.

We gratefully acknowledge the contribution of Mark Dahl and John Swinson for help in data taking, and Julie Mitchell, John Rixon and the Extrion applications laboratory staff for their diligence in processing the wafers. We also thank Alden Long for his help in the customization of the scan patterns. Carl Russo and Charles McKenna participated in several helpful discus-

sions. SIMS analysis was performed by Charles Evans Associates.

References

- [1] D.R. Myers, R.G. Wilson and J. Comas, *J. Vac. Sci. Technol.* 16 (1979) 1893.
- [2] J.F. Ziegler and R.F. Lever, *Appl. Phys. Lett.* 46 (1985) 385.
- [3] M. Miyake, M. Yoshizawa and H. Harada, *J. Electrochem. Soc.* 130 (1983) 716.
- [4] M.I. Current, N.L. Turner, T.C. Smith and D. Crane, *Nucl. Instr. and Meth. B6* (1985) 336.
- [5] N.L. Turner, M.I. Current, T.C. Smith, D. Crane, and R. Simonton, *Advanced Applications of Ion Implantation*, SPIE 530 (1985) 55.
- [6] N.L. Turner, *Nucl. Instr. and Meth.* 189 (1981) 311.
- [7] R.T. Blunt, I.R. Sanders and J.F. Singleton, *Ion Implantation Equipment and Techniques*, eds., H. Ryssel and H. Glawischnig (Springer, Berlin, 1983) p. 443.
- [8] T.M. Liu and W.G. Oldham, *IEEE Electron Devices Lett.* EDL-4 (1983) 59.
- [9] A.E. Michel, R.H. Kastl, S.R. Mader, B.J. Masters and J.A. Gardner, *Appl. Phys. Lett.* 44 (1984) 404.
- [10] P.R. Hanley and C.D. Ehrlich, *IEEE Trans. Nucl. Sci.* NS-28 (1981) 1747.
- [11] R. Liebert, B. Pedersen, C. Ehrlich and W. Callahan, *Nucl. Instr. and Meth. B6* (1985) 16.
- [12] C. Ehrlich, A. Delforge and R. Liebert, *Nucl. Instr. and Meth. B6* (1985) 228.